Electrochemical Behavior of Ba^{2+} at Liquid Metal Cathodes in Molten Chlorides

Masahiko Matsumiya, Masatoshi Takano, Ryuzo Takagi[a], and Reiko Fujita[b]

Japan Atomic Energy Research Institute, Tokai-mura, Naka-gun, Ibaraki-ken, 319-1195, Japan
[a] Research Laboratory for Nuclear Reactors, Tokyo Institute of Technology, O-okayama, Meguro-ku, Tokyo 152-8550
[b] Nuclear Engineering Laboratory, Toshiba Corporation, Ukishima-cho, Kawasaki-ku, Kawasaki 210-0862

Reprint requests to Prof. M. M.; Fax: 81 29 2825922, E-mail: matsumiya@molten.tokai.jaeri.go.jp

Z. Naturforsch. **54 a,** 739–746 (1999); received September 13, 1999

The electrochemcal behavior of Ba^{2+} on several liquid metal electrodes (Al, Bi, Cd, Pb, Sn and Zn) in a NaCl-KCl equimolar solvent at 1000 K has been investigated by means of cyclic voltammetry and chronopotentiometry. The kinetic parameters and the diffusion coefficient for Ba^{2+} were determined by cyclic voltammetry with conventional, semi-integral, semi-differential methods and chronopotentiometry. It was revealed that on a liquid Pb electrode in the NaCl-KCl system at 1000 K the quasi-reversible cathodic reaction $Ba^{2+} + 2e^- + Pb \rightarrow BaPb$ takes place. In addition, the kinetic parameters and the diffusion coefficient agree well with the values determined by various electroanalyses. The possibility of alloy formation between Ba and Sn was also demonstrated in this paper.

Key words: Alloy Formation Reaction; Barium; Liquid Metal Cathodes; Molten Salts.

1. Introduction

The electrochemical behavior of Ba^{2+} at liquid metallic cathodes in molten chloride systems is worth investigating because of its importance in nuclear engineering. For the Integral Fast Reactor (IFR) concept of Argonne National Laboratory [1 - 3] we have made proposals. The IFR concept contains a sophisticated idea of pyrochemical reprocessing in the nuclear fuel cycle. It is convenient to recover fission products like alkali and alkaline-earth elements in the salt phase in order to use the salt bath repeatedly. However, it is difficult to recover these elements from the salt bath because of their more negative reduction potentials [4] than those of the components of the solvent. Our laboratory has already examined the alloy formation reaction for Eu^{2+}, Sr^{2+} [5] and Cs^+ [6] on the liquid Pb electrode in chloride and fluoride systems. We have demonstrated that the alloy formation reaction for Eu^{2+} and Sr^{2+} is a quasi-reversible reaction at 1073 K. For Ba^{2+} [7] we have reported that the order of the thermodynamic characteristics and activity coefficients for various cathodes is consistent with the tendency of the selectivity in our results because the partial molar excess Gibbs energy and the activity coefficient correspond to the miscibility of Ba in each liquid metal. Although the diffusion coefficients of alkaline-earth elements on liquid metallic electrodes were determined by electrochemical measurements [8], the electrochemical behavior of Ba^{2+} on other liquid metallic cathodes was not revealed. We therefore selected Al, Bi, Cd, Pb, Sn and Zn as liquid metallic cathodes.

2. Experimental

(a) Melt Preparation

The chloride reagents were NaCl (Wako Chem. Ind. Ltd.: > 99.5%), KCl (Kanto Chem. Ind. Ltd.: > 99.5%) and $BaCl_2$ (Wako Chem. Ind. Ltd.: > 99.5%). Equal molar amounts of finely crushed NaCl and KCl and introduced in a quartz cell. The mixture was dehydrated by heating under vacuum at 973 K for about 7 h and then melted at 1073 K. The solute was also introduced in a quartz cell and dehydrated by heating under vacuum at about 673 K for about 24 h. The metal reagents used as liquid electrodes were Al

0932–0784 / 99 / 1200–0739 $ 06.00

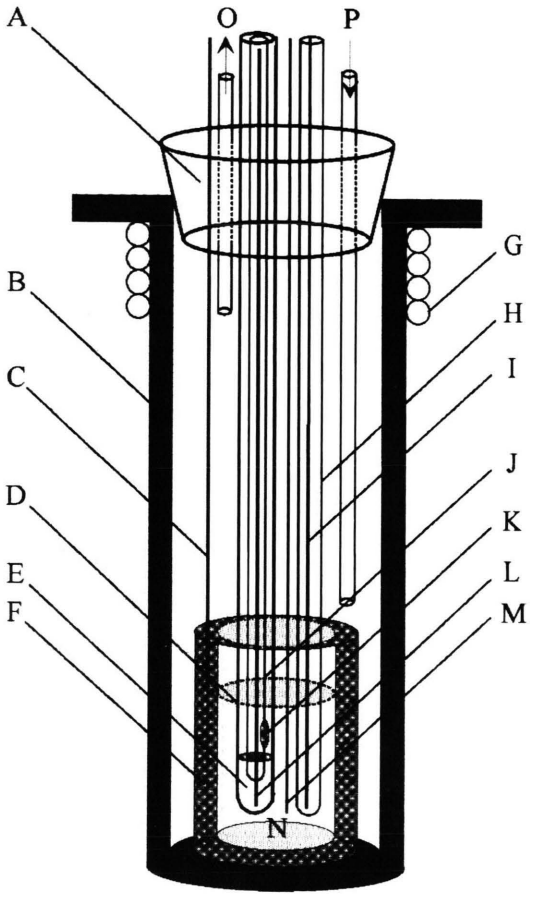

Fig. 1. The furnace cell assembly used in electrochemical measurements A: Silicon stopper, B: Stainless steel cell, C: Tungsten wire (lead to crucible), D: Quartz tube (covering the liquid electrode), E: Liquid metallic working electrode (Al, Bi, Cd, Pb, Sn and Zn), F: Graphite crucible (counter electrode), G: Cooling water, H: Quartz tube (covering thermocouple), I: Thermocouple, J: Quartz tube (covering tungsten wire), K: 6mm ø hole, L: Tungsten wire (lead to liquid metal), M: Pt wire (quasi-reference electrode), N: Molten salt (NaCl-KCl equimolar mixture), O: Ar gas outlet, P: Ar gas inlet.

(Wako Chem. Ind. Ltd.: > 99.9%), Bi (Nilaco Co.: > 99.999%), Cd (Wako Chem. Ind. Ltd.: > 99.9%), Pb (Wako Chem. Ind. Ltd.: > 99.9%), Sn (Wako Chem. Ind. Ltd.: > 99.9%) and Zn (Kanto Chem. Co.: > 99.9%).

(b) Electrodes and Electrical Devices

The furnace cell assembly is shown in Figure 1. The quasi-reference electrode was a Pt wire (1.5 mmø, Nilaco Co.: > 99.98%). Platinum makes no alloy with Ba and alkali metals. Platinum exhibits high electrochemical stability and its practical oxidation potential was close to the value at which chlorine gas evolves. The electrode was rinsed in a 1N HCl solution and degreased with acetone before experiments. Before the electrochemical experiments, pre-electrolysis was carried out with a graphite electrode under a constant current then quitted before the deposition of the bath. A graphite crucible (MS-G, Tokai Carbon: > 99.9%) was used as a counter electrode. A tungsten lead wire was connected to this crucible with ceramic binder. Six different liquid electrodes (Al: m. p. 933.4 K, Bi: m. p. 544.3 K, Cd: m. p. 593.9 K, Pb: m. p. 600.5 K, Sn: m. p. 504.97 K and Zn: m. p. 692.6 K) were used as working electrodes. They were prepared as follows. About 5 g of the metal which were introduced in the quartz tube (7.5 mm inside diameter) which had a hole of 6 mm diameter about 2.5 cm above its bottom. A tungsten lead wire was almost covered by the quartz (2.5 mm inside diameter) and only the bottom edge of the tungsten wire was immersed into the liquid metals covered by the quartz tube to prevent detection of the reaction on the tungsten wire in the melt bath. This liquid electrode was kept over the melt during pre-electrolysis. After the pre-electrolysis, this electrode was immersed into the bath. Then we carried out the electrochemical measurement with a potentio/galvanostat (Type 2001, Toho Tech.).

3. Results and Discussion

The cyclic voltammogram and chronopotentiogram of Ba^{2+} were made on a liquid metallic cathode in order to obtain the kinetic parameters and diffusion coefficients by conventional, semi-integral and semi-differential methods. The derived properties are compared with each other as follows.

(a) Conventional Electroanalysis of a Series of Voltammograms

Typical cyclic voltammograms for Ba^{2+} and no Ba^{2+} on a liquid Pb cathode are shown in Figs. 2 and 3, respectively. In Fig. 2 there are three cathodic peaks. Peak 1 at around 0 V corresponds to the reduction of Pb^{2+}/Pb, brought about by the anodic dissolution. Additionally, it is conjectured that peak 2 indicates the alloy formation reaction between Ba and Pb, since Fig. 3 which shows no peak except for the reduction of Pb^{2+}/Pb.

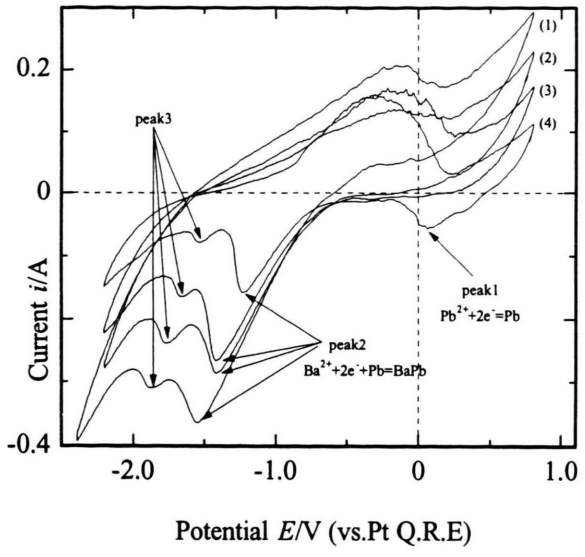

Fig. 2. Cyclic voltammogram for $BaCl_2$ on a liquid Pb electrode in the NaCl-KCl equimolar mixture at 1000 K. Sweep rates: run (1) 0.2 V/s, run (2) 0.1 V/s, run (3) 0.05 V/s, run (4) 0.01 V/s.

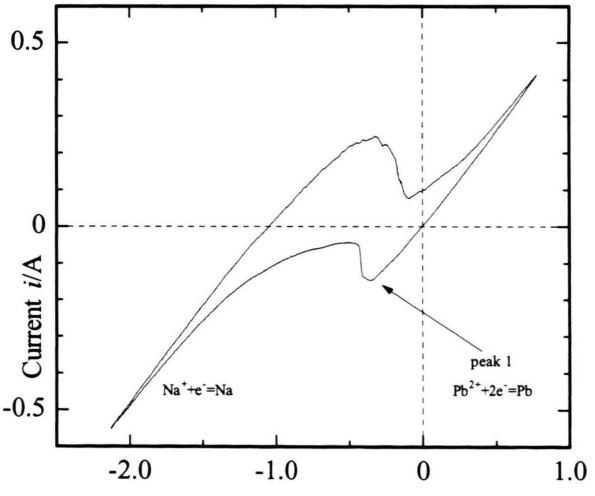

Fig. 3. Cyclic voltammogram for the NaCl-KCl system on a liquid Pb cathode at 1000 K, sweep rate: 0.1 V/s.

Probably we are dealing with an irreversible system rather than a reversible one because the cathodic peak potential is slightly shifted to the negative side on increasing the sweep rate, and the ohmic drop is large. Therefore we applied for peak 2 in Fig. 2 the relation for conventional electroanalysis of

Table 1. The kinetic parameters and the diffusion coefficient for Ba^{2+} on the liquid Pb electrode in the NaCl-KCl system at 1000 K from the various electroanalysis.

αn_a *	$k^0 \times 10^6$ (m/s) **	$D \times 10^9$ (m^2/s) *	Method
0.86±0.04	—	1.3±0.2	CV (conventional)
0.92±0.03	1.7±0.5	1.1±0.3	CV (semi-integral)
0.84±0.04	—	1.2±0.3	CV (semi-different.)
0.87±0.06	2.2±0.4	1.0±0.2	CP
		1.08±0.16	CP [8]

* The errors of αn_a and D are due to the potential and current in CV and CP. ** The error of k^0 is due to the least square method.

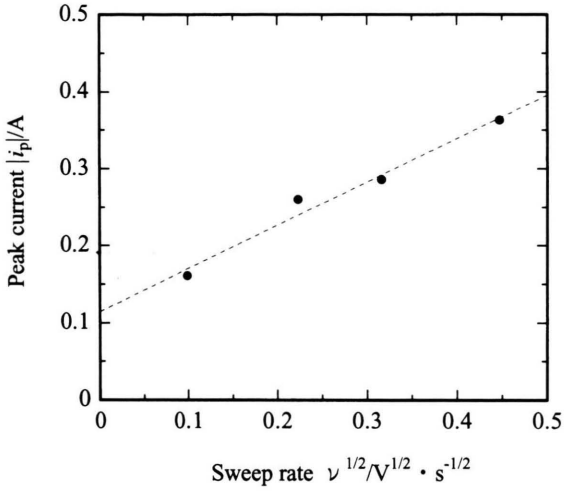

Fig. 4. Relationship between the square root of sweep rate and peak current.

a voltammogram [9],

$$\ln i_p = \frac{\alpha n_a F}{RT}(E_p - E_{1/2}) \qquad (1)$$

$$+ \ln(0.227 \times 10^{-3} \times N_a F A C^* k),$$

where i_p is the peak current, E_p the peak potential, $E_{1/2}$ the half wave potential, α a transfer coefficient, k^0 is the standard rate constant, F the Faraday constant, a the surface area of the working electrode and C^* the bulk concentration. According to (1), αn_a is calculated from the slope of the plot of $\ln i_p$ vs. $E_p - E_{1/2}$. In addition, we determined the diffusion coefficient D by the relation [9]

$$i_p = 0.4958 \times 10^{-3} n_a F A C^* D^{1/2} \nu^{1/2} \frac{\alpha n_a F}{RT}^{1/2}, \qquad (2)$$

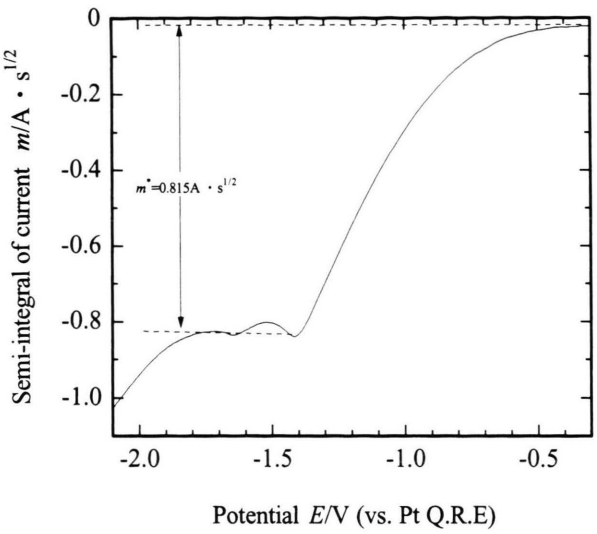

Fig. 5. Semi-integral curve plotted for $BaCl_2$ on a liquid Pb cathode in the NaCl-KCl system at 1000 K. Sweep rate: 0.05 V/s.

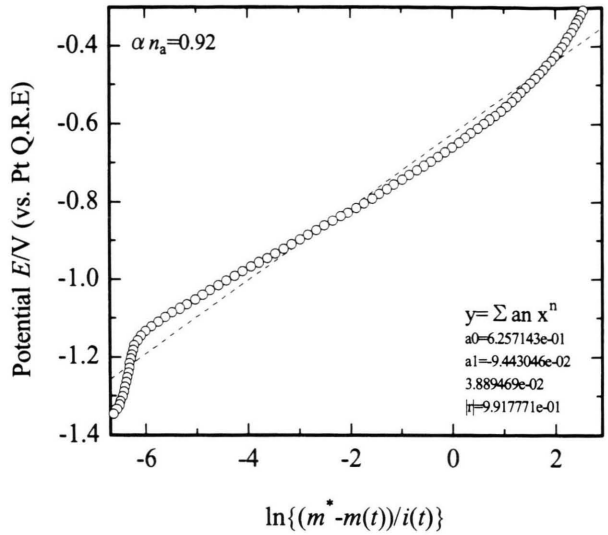

Fig. 6. Logarithmic analysis of the semi-integral of the curve plotted for $BaCl_2$ on the liquid Pb electrode in the NaCl-KCl system at 1000 K.

where ν is the sweep rate. The resultant value is listed in Table 1. For the observed cathodic peak, we assumed that $n_a = 2$ electrons are transferred. We plotted the variations of the peak currents vs. the square root of the sweep rates from 0.01 to 0.2 V/s in Figure 4. The peak currents were found to be almost proportional to the square root of the sweep rates. Therefore it is concluded that the overall reaction is controlled by diffusion. The other conventional electroanalysis, as for the width between the reduction peak and the oxidation peak, could not be applied to peak 2 because there is no anodic peak corresponding to the reduction peak, as shown in Figure 2. Therefore we determined the kinetic parameters by applying semi-integral and semi-differential electroanalysis aa discussed in the following.

(b) Semi-integral and Semi-differential Electroanalysis of the Cathodic Voltammogram

As mentioned, we calculated the kinetic parameters by considering an irreversible system. A typical semi-integral curve (Fig. 5) obtained from a linear sweep voltammetric experiment with $\nu = 0.05$ V/s (Fig. 2, run 3) yields a semi-integral limiting current, $m* = 0.815$ A·s$^{1/2}$ for the liquid Pb electrode. The occurrence of a plateau in the region of the cathodic potential proves that the rate of transfer is limited by diffusion; the plateau height is given by [10 - 13].

$$m^* = n_a F A C \sqrt{D}, \tag{3}$$

Assuming that the number of electron transferred is 2, this equation enables us to calculate the diffusion coefficient of Ba^{2+} in this melt. The calculated diffusion coefficients are listed in Table 1. In addition, by adopting the equation

$$E = E^0 + \frac{RT}{\alpha n_a F} \ln \frac{k^0}{D^{1/2}} + \frac{RT}{\alpha n_a F} \ln \frac{m^* - m(t)}{i(t)} \tag{4}$$

to the alloy formation peak as irreversible system, we evaluated the kinetic parameters. In (4) E is the apparent standard potential, E^0 the equilibrium potential of alloy formation, m a semi-integral value calculated from the current as a function of time t, and i the current. According to (4), a plot of E vs. $\ln\{(m^* - m(t))/i(t)\}$ gives a straight line having a slope of $RT/\alpha n_a F$. A typical example is shown in Fig. 6 with 0.05 V/s. The calculated kinetic parameters are also listed in Table 1.

In semi-differential electroanalysis which provides a clearer peak than the conventional cyclic voltammogram, the kinetic parameters can be obtained from the equations (5a) for the peak width W_p and (5b) for the peak height e_p [14 - 16].

$$W_p = \frac{2.94\,RT}{\alpha n_a F}, \tag{5a}$$

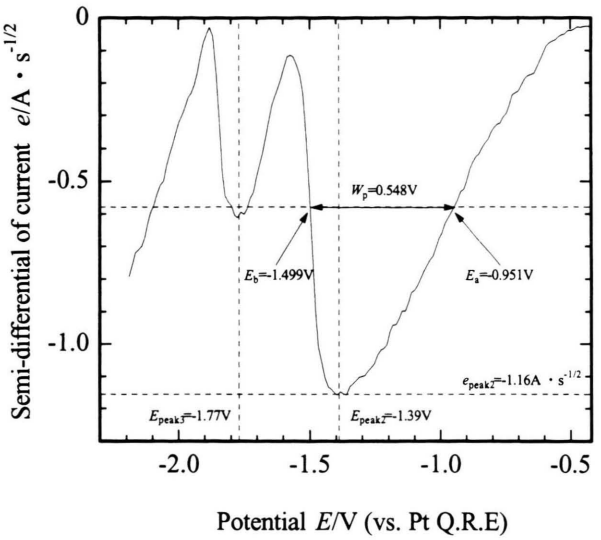

Fig. 7. Semi-differential curve plotted for $BaCl_2$ on a liquid Pb cathode in the NaCl-KCl system at 1000 K, sweep rate: 0.1 V/s.

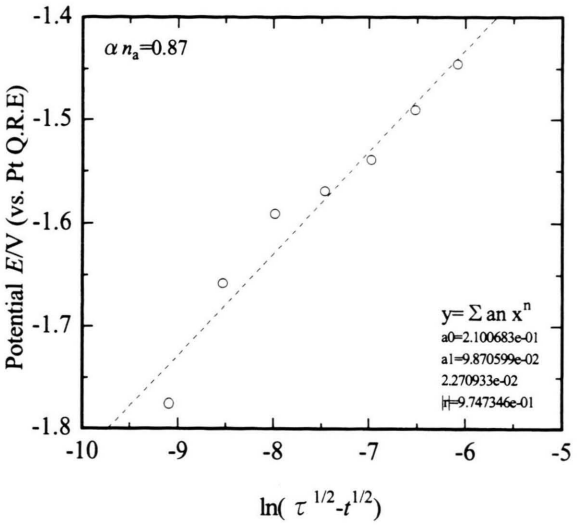

Fig. 9. Logarithmic analysis of the chronopotentiogram for $BaCl_2$ on the liquid Pb electrode in the NaCl-KCl system at 1000 K.

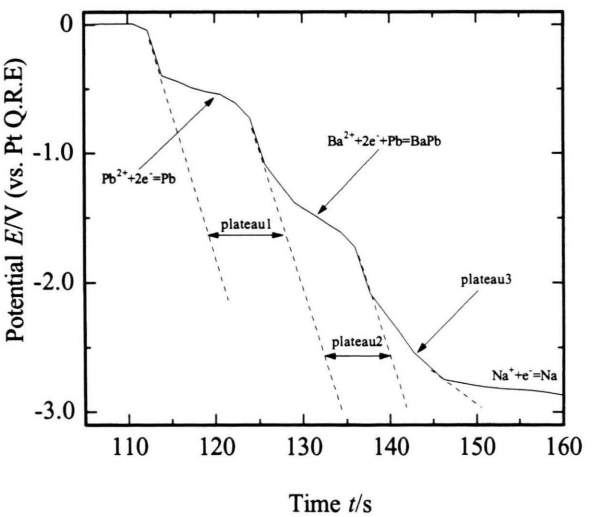

Fig. 8. Chronopotentiogram for $BaCl_2$ on the liquid Pb electrode in the NaCl-KCl system at 1000 K, cathodic current density; -0.6×10^4 A/m^2.

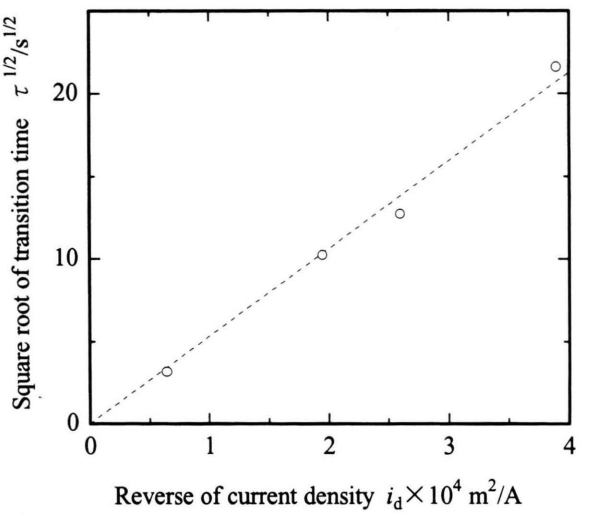

Fig. 10. Relationship between the square root of the transition time and the reverse of the current density.

$$e_p = \frac{\alpha n_a^2 F^2 A \nu C^* \sqrt{D}}{3.367\,RT}. \qquad (5b)$$

A typical semi-differential curve obtained from the semi-integral curve is shown in Figure 7. The observed peak width W_p = 0.548 V gives the kinetic parameter αn_a = 0.84. The diffusion coefficient obtained by (5b) is listed in Table 1.

(c) General Features and Characterization of the Chronopotentiometric Electroanalysis

All these features for Ba can also be depicted on the chronopotentiogram of Figure 8. A series of chronopotentiograms on a liquid Pb electrode for various current densities has also been examined. Using the equation

$$E = E^0 + \frac{RT}{\alpha n_a F} \ln \frac{2k^0}{(\pi D)^{1/2}} + \frac{RT}{\alpha n_a F} \ln(\tau^{1/2} - t^{1/2}), \quad (6)$$

αn_a was calculated from the slope of E *vs.* $\ln(\tau^{1/2} - t^{1/2})$ plots, as shown in Figure 9. This method yields $\alpha n_a = 0.87$, which is reasonably similar to its values determined by cyclic voltammogram, as shown in Table 1. The diffusion coefficients of Ba^{2+} in this melt, calculated from Sand's law [17] and the standard rate constant, which is extrapolated to $\ln(\tau^{1/2} - t^{1/2}) = 0$, are summarized in Table 1. The kinetic parameters and diffusion coefficients agree well with the values determined from the various electroanalyses. The diffusion coefficient is also in reasonable agreement with the value of $1.08 \pm 0.16 \times 10^{-9}$ m^2/s reported by Volkovich [8].

The chronopotentiometric determinations showed that the Sand product was constant, i. e., the square root of the transition time was found to be almost proportional to the reverse of the current density in Figure 10. Therefore it is concluded that the overall reaction is controlled by diffusion.

(d) Cathodic Behavior of Ba^{2+} in the Molten NaCl-KCl System

For liquid Al, Bi, Cd, and Zn electrodes there were found no alloy formation peaks and plateaus in the reduction part of cyclic voltammograms and chronopotentiograms. However, in the case of liquid Pb and Sn electrodes, we observed several cathodic peaks in voltammograms, as shown in Figs. 2 and 11, respectively. A typical cyclic voltammogram for no Ba^{2+} on a liquid Sn cathode is shown in Figure 12. The second cathodic peak around –1.5 V at 0.05 V/s in Fig. 2 was observed, and it was somewhat irreversible since the peak positions depend on the sweep rates. The cathodic limit around –2.0 V corresponds to the deposition of solvent, i. e., the reduction of Na^+/Na. According to the Ba-Pb phase diagram [18] in this condition at 1000 K, the second peak can be attributed to the reduction of Ba^{2+}, and this alloy formation reaction is considered to be the reaction

$$Ba^{2+} + 2e^- + Pb \rightarrow BaPb. \quad (7)$$

The Nernst equation for reaction (7) gives

$$E_{Ba^{2+}/Ba} = E^0_{Ba(Pb)} + \frac{RT}{2F} \ln \frac{a_{Ba^{2+}}}{a_{Ba(Pb)}}, \quad (8)$$

where $E_{Ba^{2+}/Ba}$ is the apparent standard potential of Ba, $E^0_{Ba(Pb)}$ the equilibrium potential of Ba-Pb alloy, $a_{Ba^{2+}}$ the activity of Ba in the melt, and $a_{Ba(Pb)}$ the activity of the Ba-Pb alloy. It is possible to shift $E_{Ba^{2+}/Ba}$ to more positive values by decreasing the activity of the deposited metal in (8).

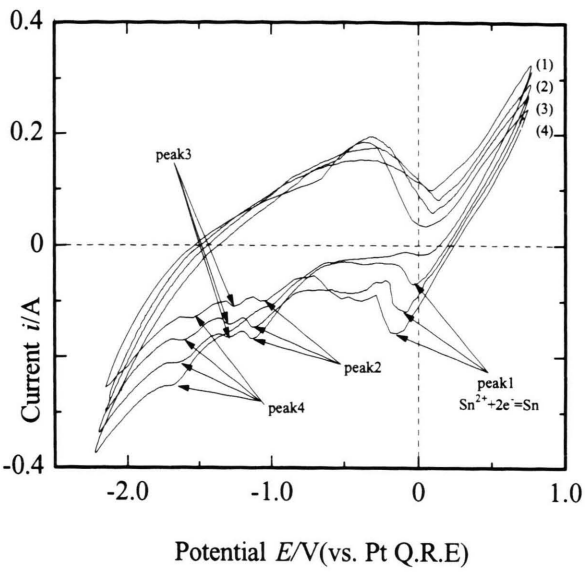

Fig. 11. Cyclic voltammogram for $BaCl_2$ on liquid Sn electrode in the NaCl-KCl equimolar mixture at 1000 K, sweep rates: run (1) 0.4 V/s, run (2) 0.2 V/s, run (3) 0.1 V/s, run (4) 0.05 V/s.

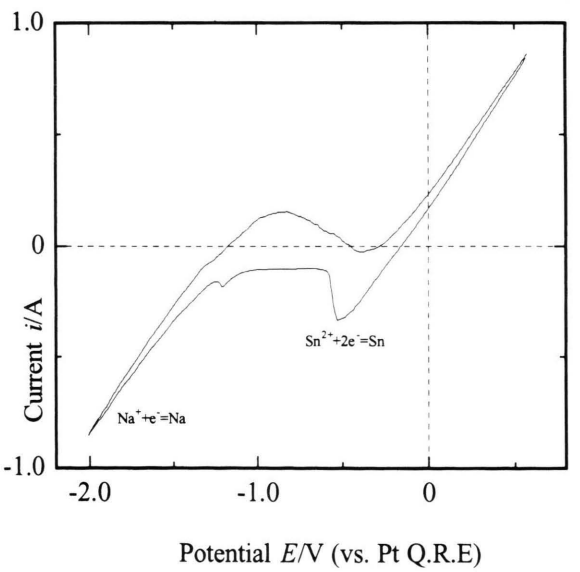

Fig. 12. Cyclic voltammogram for the NaCl-KCl system on a liquid Sn cathode at 1000 K, sweep rate: 0.1 V/s.

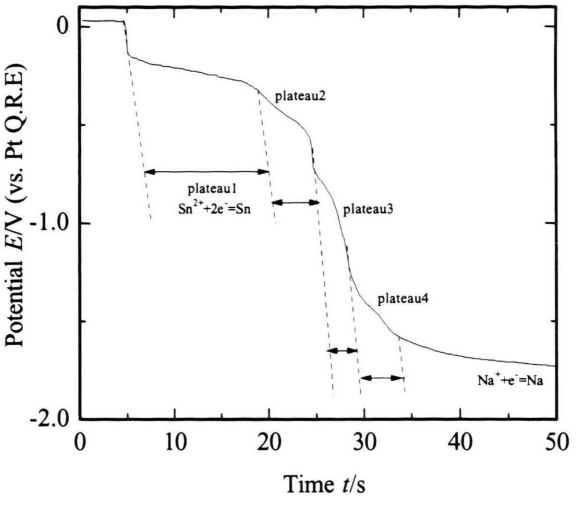

Fig. 13. Chronopotentiogram for $BaCl_2$ on the liquid Sn electrode in the NaCl-KCl system at 1000 K, cathodic current density; -0.6×10^4 A/m^2.

The chronopotentiogram of $BaCl_2$ in NaCl-KCl shows that the plateau around –0.5 V corresponds to the deposition of Pb, and the peak around –1.5 V corresponds to the alloy formation of Ba on a liquid Pb cathode, followed by the deposition of solvent Na around –2.8 V, as shown in Figure 8. On the other hand, in case of a liquid Sn electrode, there are several cathodic plateaus in the chronopotentiongrams, as shown in Figure 13. The peak 1 in Fig. 12 and the plateau 1 in Fig. 13 correspond to the reduction of Sn^{2+}. Fom the phase diagram at [19 - 22], we could not confirm the formation of an alloy between Ba and Sn because the phase diagram is not well defined at this temperature. However, it is conjectured by comparison with Figs. 11 and 12 that the decomposition mechanism of Ba^{2+} is related to Ba-Sn alloy formation. It is difficult to apply these small cathodic peaks and plateaus in Figs. 11 and 13 to the above electroanalytical methods. However, each plateau in a chronopotentiogram corresponds to a peak in the voltammogram.

The standard rate constants determined by various electroanalyses agree well with the values obtained by linear sweep voltammetry and by semi-integral electroanalysis. These values obey the Matsuda and Ayabe criterion [23] for a quasi-reversible system,

$$2.0\times10^{-7}(n_a\nu)^{1/2} < k^0 < 0.3\times10^{-2}(n_a\nu)^{1/2} \quad (9)$$

(Quasi-reversible),

which yields in our conditions

$$8.6\times10^{-8} < k^0 < 7.0\times10^{-4} \quad (10)$$

(Quasi-reversible).

Thus, the alloy formation reaction of Ba-Pb can be qualified as quasi-reversible at 1000 K.

4. Conclusion

In order to show the possibility of alloy formation between Pb and Ba, the electrochemical reduction reaction of Ba^{2+} on several liquid metallic cathodes in the NaCl-KCl system was investigated. The results allow us to conclude that an alloy is formed by the reaction $Ba^{2+} + 2e^- + Pb \rightarrow BaPb$ on liquid Pb cathode. It was also clarified that this alloy formation is quasi-reversible at 1000 K Additionally, the kinetic parameters and the diffusion coefficient show good agreement with the values determined by the various electroanalyses.

[1] Y. I. Chang, L. C. Walters, J. E. Battles, D. R. Pederson, D. C. Wade, and M. J. Lineberry, ANL-IFR-125 (1990).
[2] Y. I. Chang et al., ANL-IFR-149 (1991).
[3] Y. I. Chang et al., ANL-IFR-246 (1994).
[4] W. J. Hamer, M. S. Malmberg, and B. Rubin, J. Electrochem. Soc., **112**, 750 (1965).
[5] M. Matsumiya, R. Takagi, and R. Fujita, J. Nucl. Sci. Technol. **34**, 310 (1997).
[6] M. Matsumiya, R. Takagi, and R. Fujita, J. Nucl. Sci. Technol. **35**, 137 (1998).
[7] M. Matsumiya, M. Takano, R. Takagi, and R. Fujita, J. Nucl. Sci. Technol. **35**, 836 (1998).
[8] A. V. Volkovich, Melts **7**, 106 (1994).
[9] R. S. Nicholson and I. Shain, Anal. Chem. **36**, 706 (1964).
[10] K. B. Oldham, J. Electroanal. Chem. **26**, 331 (1970).
[11] M. Grenness and K. B. Oldham, Anal. Chem. **44**, 1121 (1972).
[12] M. Goto and K. B. Oldham, Anal. Chem. **45**, 2043 (1973).
[13] K. B. Oldham, Anal. Chem. **44**, 196 (1972).
[14] P. Dalrymple-Alford, M. Goto, and K. B. Oldham, J. Electroanal. Chem. **85**, 1 (1977).
[15] M. Goto and D. Ishii, J. Electroanal. Chem. **61**, 361 (1975).

[16] K. B. Oldham, J. Electroanal. Chem. **121**, 341 (1981).
[17] A. J. Bard and L. R. Faulkner, 'Electrochemical Methods, Fundamentals and Applications', John Wiley and Sons, New York 1980, p. 253.
[18] T. B. Massalski, 'Binary Alloy Phase Diagrams, Amer. Soc. Metals 1986, Vol 1'.
[19] K. W. Ray and R. G. Thompson, Metals Alloys **1**, 314 (1930).
[20] W. Rieger and E. Parthe, Acta Crystallogr. **22**, 919 (1967).
[21] W. Dorrshield, A. Widera, and A. Schäfer, Z. Naturforsch. **32b**, 1097 (1977).
[22] G. Bruzzone, E. Franceschi, and F. Merlo, J. Less Common Met. **60**, 59 (1978).
[23] H. Matsuda and Y. Ayabe, Z. Electrochem. **59**, 494 (1955).